CELL CYCLE
2017, VOL. 16, NO. 11, 1063–1069
https://doi.org/10.1080/15384101.2017.1314406

Taylor & Francis
Taylor & Francis Group

REPORT

Combination of gemcitabine and docetaxel regresses both gastric leiomyosarcoma proliferation and invasion in an imageable patient-derived orthotopic xenograft (iPDOX) model

Kei Kawaguchi[a,b,c], Kentaro Igarashi[a,b], Takashi Murakami[a,b], Tasuku Kiyuna[a,b], Scott D. Nelson[d], Sarah M. Dry[d], Yunfeng Li[d], Tara A. Russell [e], Arun S. Singh[f,g], Bartosz Chmielowski [f], Michiaki Unno[c], Fritz C. Eilber [e,g], and Robert M. Hoffman[a,b,g]

[a]AntiCancer, Inc., San Diego, CA, USA; [b]Department of Surgery, University of California, San Diego, CA, USA; [c]Department of Surgery, Graduate School of Medicine, Tohoku University, Sendai, Japan; [d]Department of Pathology, University of California, Los Angeles, CA, USA; [e]Division of Surgical Oncology, University of California, Los Angeles, CA, USA; [f]Division of Hematology-Oncology, University of California, Los Angeles, CA, USA; [g]PDOX Inc., San Diego, CA, USA

ABSTRACT

Gastric leiomyosarcoma is a recalcitrant cancer and the chemotherapy strategy is controversial. The present study used a patient-derived orthotopic xenograft (PDOX) nude mouse model of gastric leiomyosarcoma to identify an effective therapeutic regimen to develop individualized precision medicine for this disease. The gastric leiomyosarcoma obtained from a patient was first grown in transgenic nude mice ubiquitously expressing red fluorescent protein (RFP) to stably label the tumor stroma. The RFP-expressing tumor was then passaged orthotopically in the gastric wall of non-transgenic nude mice to establish an imageable PDOX (iPDOX) model. The bright fluorescent tumor was readily imaged over time to determine drug efficacy. Four weeks after implantation, 70 PDOX nude mice were divided into 7 groups: control without treatment (n = 10); doxorubicin (DOX) (2.4 mg/kg, intraperitoneally (i.p.), once a week for 2 weeks, n = 10); gemcitabine (GEM)/ docetaxel (DOC) (GEM: 100 mg/kg, DOC: 20 mg/kg, i.p., once a week for 2 weeks, n = 10); cyclophosphamide (CPA) (140 mg/kg, i.p., once a week for 2 weeks, n = 10); temozolomide (TEM) (25 mg/kg, orally, daily for 14 consecutive days, n = 10); yondelis (YON) (0.15 mg/kg, i.v., once a week for 2 weeks, n = 10); pazopanib (PAZ) (100 mg/kg, orally, daily for 14 consecutive days, n = 10). On day 14 from initiation of treatment, all treatments except PAZ significantly inhibited tumor growth compared with untreated control (DOX: $p < 0.01$, GEM/DOC: $p < 0.01$, CPA: $p < 0.01$, TEM: $p < 0.01$, YON: $p < 0.01$) on day 14 after initiation. In addition, only GEM/DOC was more significantly effective than DOX ($p < 0.05$). GEM/DOC could regress the leimyosarcoma in the PDOX model and has important clinical potential for precision individual treatment of leiomyosarcoma patients.

ARTICLE HISTORY
Received 27 January 2017
Revised 23 March 2017
Accepted 27 March 2017

KEYWORDS
docetaxel; drug-response; gemcitabine; gastric leiomyosarcoma; nude mice; orthotopic; PDOX; precision therapy; red fluorescent protein; tumor regression

Introduction

Leiomyosarcoma is the most common histotype of gastro-intestinal sarcoma.[1] Gastro-intestinal leiomyosarcoma originates from smooth muscle or a blood vessel[2] and is a recalcitrant disease, relatively unresponsive to chemotherapy or radiation. Currently only surgery is curative[2] and 50% of patients will develop local recurrence after tumor resection and subsequently distant metastases.[3]

Doxorubicin (DOX) and ifosfamide (IFO) are first line for sarcomas but not effective for leiomyosarcoma with a response rate of only 18%.[4] Gemcitabine (GEM) and docetaxel (DOC) have efficacy for adjuvant treatment of uterine leiomyosarcoma,[5] but efficacy has not been shown for gastrointestinal leiomyosarcoma. Yondelis (YON) has shown efficacy for leiomyosarcoma of both uterine and non-uterine origin,[6] but not yet for gastrointestinal leiomyosarcoma. The tyrosine kinase inhibitor pazopanib (PAZ) has not demonstrated significant activity against leiomyosarcoma.[7] Leiomysarcoma is heterogeneous as well as treatment resistant. Novel more effective personalized therapy is therefore needed for leiomysarcoma.

Clinically-relevant mouse models of leiomyosarcoma could enable both discovery of new treatment strategies as well as individualized precision therapy, based on each patient's tumor. Toward this goal, our laboratory pioneered the patient-derived orthotopic xenograft (PDOX) nude mouse model with the technique of surgical orthotopic implantation (SOI), including pancreatic,[8-11] breast,[12] ovarian,[13] lung,[14] cervical,[15] colon,[16-18] stomach,[19] sarcoma,[20-24] and melanoma.[25-27] The PDOX model, developed by our laboratory over the past 29 years, has many advantages over subcutaneous-transplant models which are growing ectopically under the skin.[28]

Our laboratory has also developed the imageable PDOX (iPDOX) model using fluorescent protein labeling. The

CONTACT Robert M. Hoffman all@anticancer.com AntiCancer, Inc., 7917 Ostrow Street, San Diego, CA 92111; Fritz C. Eilber fceilber@mednet.ucla.edu Prof. of Surgery, Prof. of Mol. & Medical Pharmacology UCLA, Division of Surgical Oncology, 10833 LeConte Avenue, Rm 54–140 CHS, Los Angeles, CA 90095–1782.

patient tumors were passaged orthotopically in transgenic nude mice ubiquitously expressing red fluorescent protein (RFP) or green fluorescent protein (GFP) or cyan fluorescent protein (CFP). The primary patient tumors acquired RFP-expressing stroma.[29] Subsequent liver metastases and disseminated peritoneal metastases maintained the stroma from the primary tumor, and possibly recruited additional fluorescent protein-expressing stroma, resulting in their very bright fluorescence.[30] Tumors, which acquired very bright fluorescent protein-expressing stromal cells, were then orthotopically passaged to non-transgenic nude mice. It was possible to image the brightly fluorescent tumors non-invasively longitudinally as they progressed in the non-transgenic nude mice.[31] Undifferentiated pleomorphic sarcoma (UPS) PDOX tumors, previously grown in RFP transgenic nude mice for only one passage, had very bright fluorescence and after passage to non-transgenic nude mice maintained the bright fluorescence and were non-invasively imageable.,[32,33]

A telomerase-dependent GFP-containing adenovirus OBP-401 was used to label the cancer cells of a pancreatic cancer PDOX which was previously grown in a RFP transgenic mouse that stably labeled the PDOX stroma cells bright red. This dual-color PDOX model was shown to be very effective for fluorescence-guided surgery (FGS).[34]

In the present study, we established a PDOX nude mouse model with gastric leiomyosarcoma from a patient and evaluated the efficacy of 6 drugs to find an effective treatment strategy against leiomyosarcoma tumor growth and metastasis.

Results and discussion

All treatments except for PAZ significantly inhibited tumor volume compared with untreated control; DOX: $p < 0.01$; GEM/DOC: $p < 0.01$; CPA: $p < 0.01$; TEM: $p < 0.01$; YON: $p < 0.01$; on day 14 after initiation. GEM/DOC was significantly more effective than DOX, a first-line therapy for sarcoma ($p < 0.01$) (Fig. 1, Fig. 2).

The leiomyosarcoma was grown in red fluorescent protein (RFP) transgenic mice whereby it stably acquired RFP-expressing stroma.[31,32]

Treatment efficacy in gastric leiomyosarcoma PDOX was evaluated by tumor fluorescent area and tumor fluorescence intensity. As shown in Figure 3, all treatments could significantly reduce both fluorescent tumor area and tumor fluorescence intensity compared with untreated control: fluorescent area = 72.1 ± 44.3 (mm^3); fluorescence intensity = 776644 ± 418682; DOX: fluorescent area = 22.1 ± 17.3 (mm^3), $p < 0.01$; fluorescence intensity = 256531 ± 226593, $p < 0.01$; GEM/

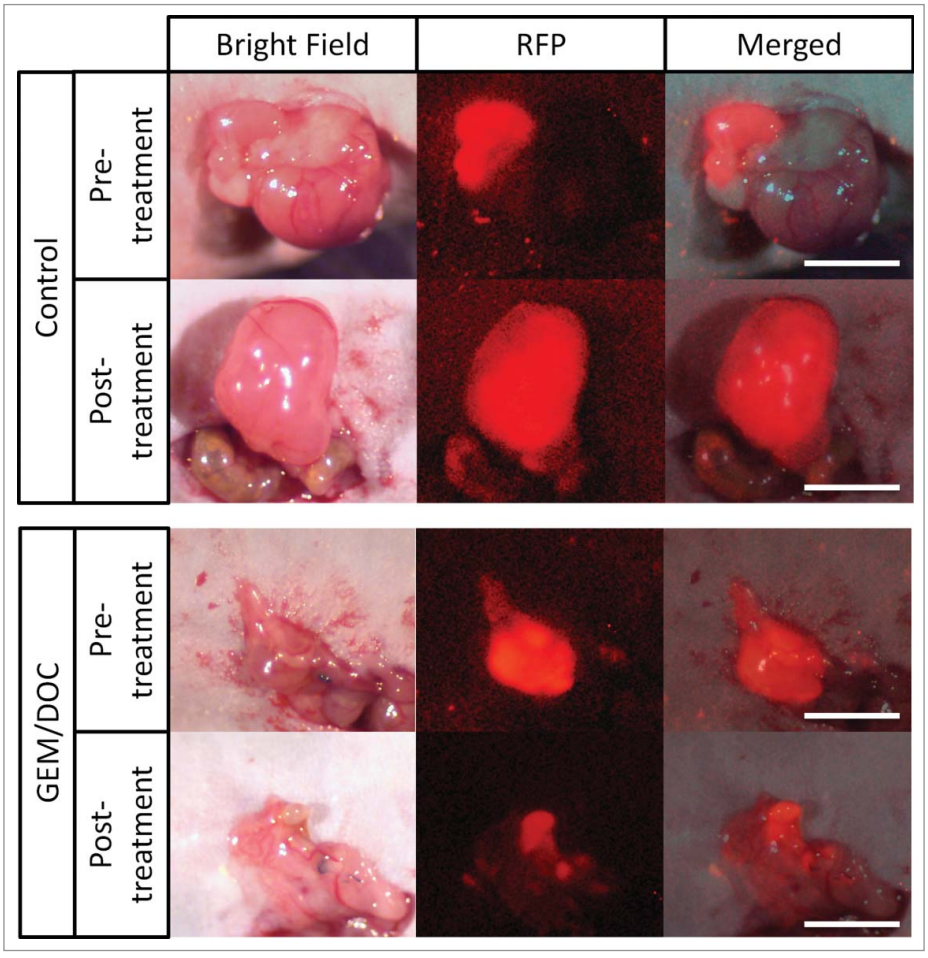

Figure 1. Imaging of drug efficacy on a leiomyosarcoma iPDOX. The PDOX model treated with GEM combined with DOC (GEM/DOC) demonstrated tumor regression. Scale bar: 5 mm.

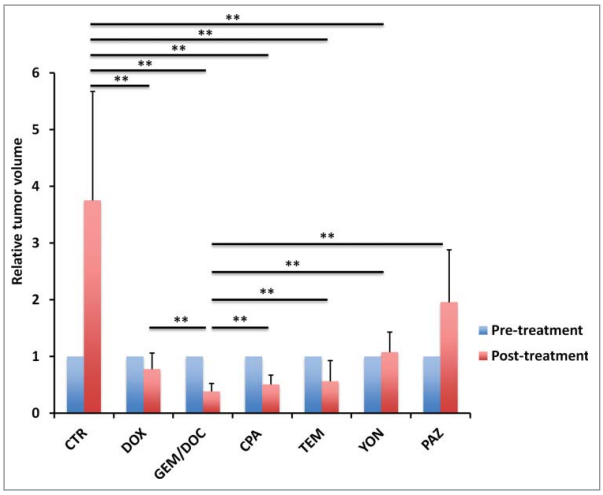

Figure 2. Efficacy of treatment on leiomyosarcoma iPDOX. Bar graph shows relative tumor volume at a post-treatment point relative to the initial pre-treatment tumor volume. All treatments except for PAZ significantly inhibited tumor growth compared with untreated control (CTR). GEM/DOC was the strongest and significantly more effective than other therapies (DOX: $p < 0.01$, CPA: $p < 0.01$, TEM: $p < 0.01$, YON: $p < 0.01$, PAZ: $p < 0.01$). $^{**}p < 0.01$. Error bars: ± SD.

DOC: fluorescent area = 8.84 ± 1.23 (mm^3), p <0.01; fluorescence intensity = 139885 ± 12081, $p < 0.01$; CPA: fluorescent area = 19.8 ± 18.0 (mm^3), $p < 0.01$; fluorescence intensity = 233161 ± 175932, $p < 0.01$; TEM: fluorescent area = 22.6 ± 15.8 (mm^3), $p < 0.01$; fluorescence intensity = 308721 ± 215154, p <0.01; YON: fluorescent area = 16.3 ± 10.1 (mm^3), p<0.01; fluorescence intensity = 216880 ± 145555, $p < 0.01$; PAZ: fluorescent area = 32.0 ± 17.2 (mm^3), $p < 0.05$; fluorescence intensity = 396556 ± 306308, $p < 0.05$. There was a strong correlation between tumor fluorescent area and fluorescence intensity ($R^2 = 0.9105$, p <0.0001) (Fig. 4).

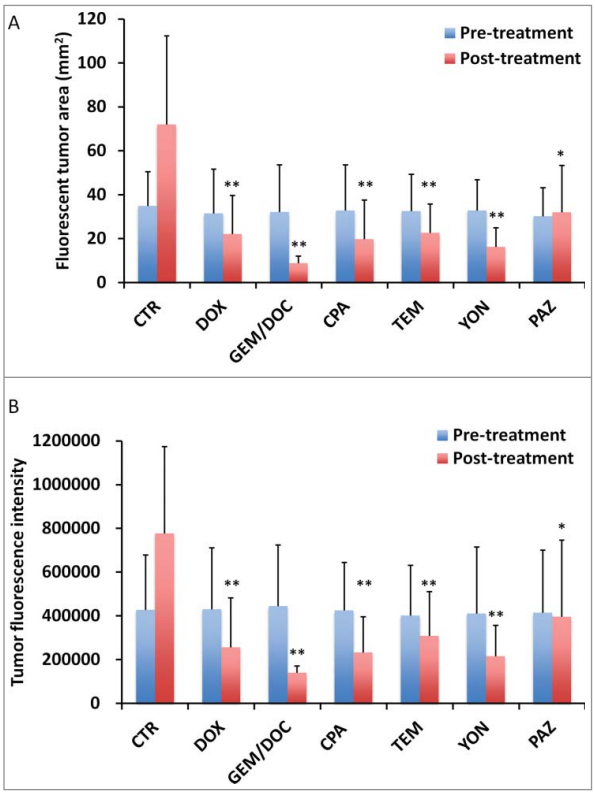

Figure 3. Treatment efficacy for leiomyosarcoma iPDOX. Bar graphs show the tumor fluorescent area (mm^2) (A) and fluorescence intensity (B). All treatments significantly inhibited the leiomyosarcoma iPDOX compared with untreated control. $^{**}p < 0.01$, $^{*}p < 0.05$. Error bars: ± SD.

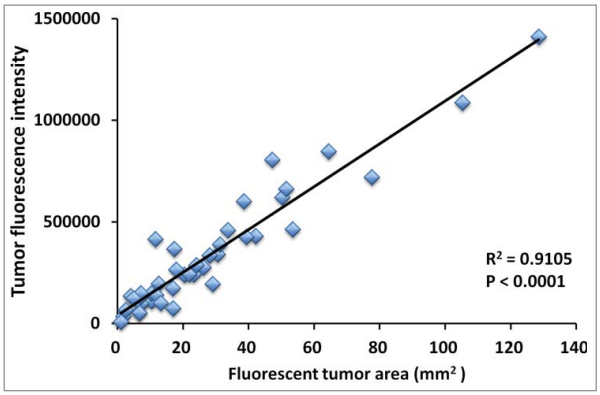

Figure 4. Correlation of tumor fluorescent area and tumor fluorescence intensity. Tumor area significantly correlated with fluorescence intensity ($R^2 = 0.9105$, $p < 0.0001$). Please see Materials and methods for details.

Tumor volume at post-treatment, relative to the initial pre-treatment tumor volume, is shown below: untreated control: 3.75 ± 1.63; DOX: 0.78 ± 0.28; GEM/DOC: 0.39 ± 0.09; CPA: 0.51 ± 0.23; TEM: 0.56 ± 0.28; YON: 1.08 ± 0.34; PAZ: 1.96 ± 0.75. Both relative tumor fluorescent area and relative fluorescence intensity showed a strong positive correlation with relative tumor volume ($R^2 = 0.8927$, p <0.0001: $R^2 = 0.8967$, $p < 0.0001$: respectively) (Fig. 5).

The relative body weight on day 14 compared with day 0 did not significantly differ between each treatment group, including untreated control (Fig. 6).

Histologically, the untreated control tumor was mainly comprised of viable cells without obvious necrosis. In contrast, the tumor treated with GEM/DOC had extensive necrosis (Fig. 7).

The DOX response rate in the clinic for leiomyosarcoma was reported as only 18%,[3] however, in the present study, DOX was effective for the gastric leiomyosarcoma PDOX. YON has shown efficacy for many types of leiomyosarcoma,[6] however, its treatment efficacy was less than GEM/DOC which showed the most efficacy in the present study.

The present study took advantage of technology we previously developed to stably label the stroma of a patient tumor by growing it in transgenic mice ubiquitously-expressing a fluorescent protein, in this case, RFP. The tumor was then passaged to non-transgenic mice which enabled high contrast imaging that showed the invasive capability of the tumor which was inhibited by effective chemotherapy. We have termed this model imageable PDOX (iPDOX) which should be highly useful for imaging tumor growth, invasion and metastasis.

Therefore, the PDOX model may be useful for precise individualized therapy, especially for rare heterogeneous sarcomas such as gastric leiomyosarcoma.[26]

Previously-developed concepts and strategies of highly selective tumor targeting can take advantage of molecular targeting of tumors, including tissue-selective therapy which focuses on unique differences between normal and tumor tissues.[35-40]

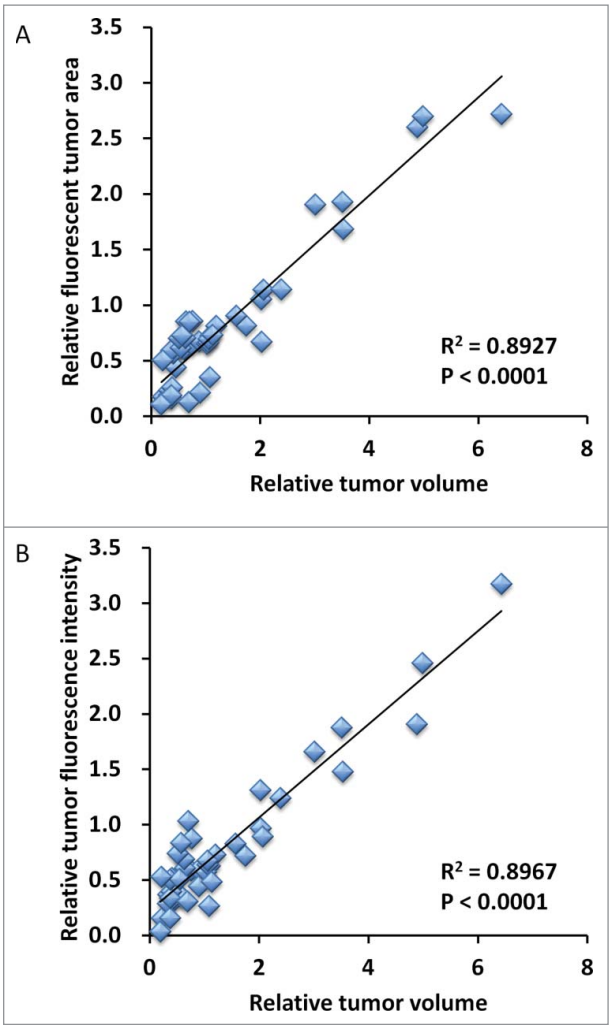

Figure 5. Correlation of fluorescence intensity and fluorescent area with tumor volume. Both relative tumor fluorescent area (A) and relative fluorescence intensity (B) demonstrated a strong positive correlation with relative tumor volume ($R^2 = 0.8927$, $p < 0.0001$; $R^2 = 0.8967$, $p < 0.0001$; respectively).

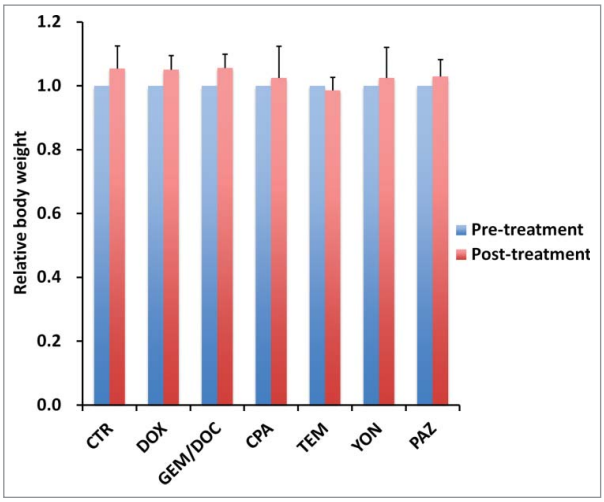

Figure 6. Effect of each treatment on mouse body weight. Bar graph shows relative body weight at post-treatment relative to the pre-treatment. There were no significant differences between each treatment group including untreated control.

Conclusions

In the present study, the iPDOX model helped identify the high efficacy of GEM combined with DOC against the gastric leiomyosarcoma. GEM/DOC caused tumor regression and arrested the invasiveness of the tumor. The PDOX model for gastric leiomyosarcoma will be further developed to identify effective individualized patient therapy.

Materials and methods

Mice

Athymic non-transgenic *nu/nu* nude mice and transgenic nude mice ubiquitously-expressing red fluorescent protein (RFP) mice (AntiCancer Inc., San Diego, CA), 4–6 weeks old, were used in this study.[41] The transgenic nude mice express the RFP gene under the control of the chicken β-actin promoter and cytomegalovirus enhancer.[42] Animals were housed in a barrier facility on a high efficacy particulate arrestance (HEPA)-filtered rack under standard conditions of 12-hour light/dark cycles. The animals were fed an autoclaved laboratory rodent diet. All mouse surgical procedures and imaging were performed with the animals anesthetized by subcutaneous injection of a ketamine mixture (0.02 ml solution 20 mg/kg ketamine, 15.2 mg/kg xylazine, and 0.48 mg/kg acepromazine maleate). The response of animals during surgery was monitored to ensure adequate depth of anesthesia. The animals were observed on a daily basis and humanely killed by CO_2 inhalation if they met the following humane end point criteria: severe tumor burden (more than 20 mm in diameter), prostration, significant body weight loss, difficulty breathing, rotational motion and body temperature drop. All animal studies were conducted in accordance with the principles and procedures outlined in the National Institutes of Health Guide for the Care and Use of Animals under Assurance Number A3873–1.

Patient-derived tumor

A patient diagnosed with gastric leiomyosarcoma had the tumor resected in the Department of Surgery, University of California, Los Angeles (UCLA). Written informed consent was provided by the patient, and the Institutional Review Board (IRB #10–001857) of UCLA approved this experiment. The patient had a highly-aggressive and high-grade gastric leiomyosarcoma that had grown to greater than 10 cm and was resected from the gastric wall in the upper abdomen. After the original tumor resection that was used for the PDOX model, the patient recurred with diffuse regional metastasis 4 months after surgery.

Establishment of PDOX models of leiomyosarcoma by surgical orthotopic implantation (SOI)

A fresh sample of gastric leiomyosarcoma of the patient was obtained and transported immediately to the laboratory at AntiCancer, Inc., on wet ice. The sample was cut into 5-mm fragments and implanted subcutaneously in nude mice. After 3 weeks, the subcutaneously-implanted tumors grew to more than 10 mm in diameter. The subcutaneously-grown tumors were cut into 5-mm fragments and implanted subcutaneously

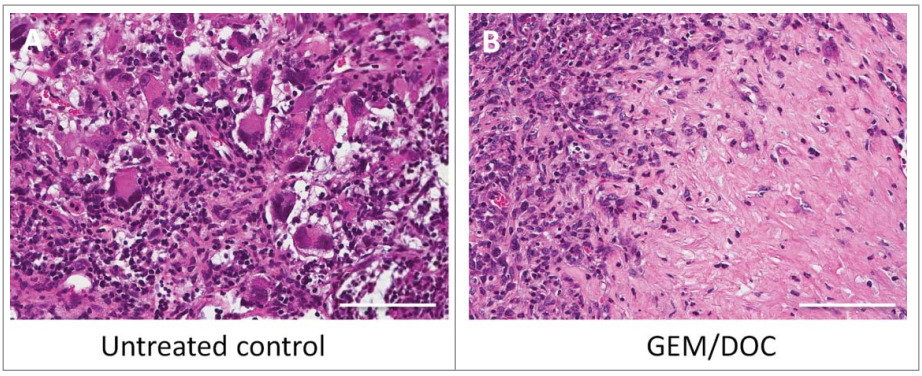

Figure 7. Histological response. A. The untreated control comprised viable cells without necrosis. B. The tumor treated with GEM and DOC exhibited necrosis. Scale bars: 100 μm.

in RFP transgenic nude mice.[41-43] After 3 weeks, the subcutaneously-implanted tumors in RFP mice were harvested and cut into small fragments (3 mm^3). After non-transgenic nude mice were anesthetized with the ketamine solution described above, a 1–2 cm skin incision was made on the middle abdomen through the skin, fascia and peritoneum and thereby the stomach was exposed. Surgical sutures (8–0 nylon) were used to implant tumor fragments onto the gastric wall to establish the PDOX model. The wound was closed with a 6–0 nylon suture (Ethilon, Ethicon, Inc., NJ, USA).[44]

Treatment study design in the leiomyosarcoma PDOX model

PDOX mouse models were randomized into 7 groups of 10 mice each: untreated control; DOX (2.4 mg/kg, i.p., qw × 2); GEM/DOC (GEM: 100 mg/kg, DOC: 20 mg/kg, i.p., qw × 2); CPA (140 mg/kg, i.p., qw × 2); TEM (25 mg/kg, p.o., qd × 14); YON (0.15 mg/kg, i.v., qw × 2); PAZ (100 mg/kg, p.o., qd × 14). Tumor length and width were measured after 14 d treatment. Tumor volume was calculated with the following formula: Tumor volume (mm^3) = length (mm) × width (mm) × width (mm) × 1/2. Data are presented as mean ± SD. The tumor volume ratio is defined as the tumor volume at a post-treatment point relative to pre-treatment tumor volume.

Imaging of the fluorescent leiomyosarcoma PDOX model

Fluorescence imaging of the macroscopic tumor was performed with the OV100 Small Animal Imaging System (Olympus, Tokyo, Japan).[45] The tumor fluorescent area and total fluorescence intensity were analyzed with UVP software (UVP, Upland, CA). Treatment efficacy was evaluated by tumor fluorescent area and tumor fluorescence intensity at post-treatment compared with at pre-treatment.[46]

Histological examination

Fresh tumor samples were fixed in 10% formalin and embedded in paraffin before sectioning and staining. Tissue sections (5 μm) were deparaffinized in xylene and rehydrated in an ethanol series. Hematoxylin and eosin (H&E) staining was performed according to standard protocols. Histological examination was performed with a BHS System Microscope (Olympus Corporation, Tokyo, Japan). Images were acquired with INFINITY ANALYZE software (Lumenera Corporation, Ottawa, Canada).[26,27]

Statistical analysis

JMP version 11.0 was used for all statistical analyses. Significant differences for continuous variables were determined using the Mann-Whitney *U* test. Line graphs expressed average values and error bar showed SD. A probability value of $P \leq 0.05$ was considered statistically significant.

Disclosure of potential conflicts of interest

No potential conflicts of interest were disclosed.

ORCID

Tara A. Russell http://orcid.org/0000-0002-3912-3601
Bartosz Chmielowski http://orcid.org/0000-0002-2374-3320
Fritz C. Eilber http://orcid.org/0000-0003-3336-9333

References

[1] McGrath PC, Neifeld JP, Lawrence W Jr, Kay S, Horsley JS 3rd, Parker GA. Gastrointestinal sarcomas. Analysis of prognostic factors. Ann Surg 1987; 206:706-10
[2] Cui RR, Wright JD, Hou JY. Uterine leiomyosarcoma: A review of recent advances in molecular biology, clinical management and outcome. BJOG 2017; https://doi.org/10.1111/1471-0528.14579
[3] Reichardt P. Soft tissue sarcomas, a look into the future: different treatments for different subtypes. Future Oncol 2014; 10(8 Suppl): s19-27; PMID:25048045; https://doi.org/10.2217/fon.14.116
[4] Oosten AW, Seynaeve C, Schmitz PI, den Bakker MA, Verweij J, Sleijfer S. Outcomes of first-line chemotherapy in patients with advanced or metastatic leiomyosarcoma of uterine and non-uterine origin. Sarcoma 2009; 2009:348910; PMID:20066161; https://doi.org/10.1155/2009/348910
[5] Hensley ML, Ishill N, Soslow R, Larkin J, Abu-Rustum N, Sabbatini P, Konner J, Tew W, Spriggs D, Aghajanian CA. Adjuvant gemcitabine plus docetaxel for completely resected stages I-IV high grade uterine leiomyosarcoma: Results of a prospective study. Gynecol Oncol 2009; 112:563-7; PMID:19135708; https://doi.org/10.1016/j.ygyno.2008.11.027
[6] Samuels BL, Chawla S, Patel S, von Mehren M, Hamm J, Kaiser PE, Schuetze S, Li J, Aymes A, Demetri GD. Clinical outcomes and safety with trabectedin therapy in patients with advanced soft tissue sarcomas following failure of prior chemotherapy: results of a worldwide

expanded access program study. Ann Oncol 2013; 24:1703-9; PMID:23385197; https://doi.org/10.1093/annonc/mds659

[7] van der Graaf WT, Blay JY, Chawla SP, Kim DW, Bui-Nguyen B, Casali PG, Schöffski P, Aglietta M, Staddon AP, Beppu Y, et al. Pazopanib for metastatic soft-tissue sarcoma (PALETTE): a randomised, double-blind, placebo-controlled phase 3 trial. Lancet 2012; 379:1879-86; PMID:22595799; https://doi.org/10.1016/S0140-6736(12)60651-5

[8] Hiroshima Y, Zhang Y, Murakami T, Maawy AA, Miwa S, Yamamoto M, Yano S, Sato S, Momiyama M, Mori R, et al. Efficacy of tumor-targeting *Salmonella typhimurium* A1-R in combination with anti-angiogenesis therapy on a pancreatic cancer patient-derived orthotopic xenograph (PDOX) and cell line mouse models. Oncotarget 2014; 5:12346-57; PMID:25402324; https://doi.org/10.18632/oncotarget.2641

[9] Fu X, Guadagni F, Hoffman RM. A metastatic nude-mouse model of human pancreatic cancer constructed orthotopically with histologically intact patient specimens. Proc Natl Acad Sci USA 1992; 89:5645-9; PMID:1608975; https://doi.org/10.1073/pnas.89.12.5645

[10] Hiroshima Y, Maawy A, Zhang Y, Murakami T, Momiyama M, Mori R, Matsuyama R, Katz MH, Fleming JB, Chishima T, et al. Metastatic recurrence in a pancreatic cancer patient derived orthotopic xenograft (PDOX) nude mouse model is inhibited by neoadjuvant chemotherapy in combination with fluorescence-guided surgery with an anti-CA 19–9-conjugated fluorophore. PLOS ONE 2014; 9:e114310; PMID:25463150; https://doi.org/10.1371/journal.pone.0114310

[11] Hiroshima Y, Maawy AA, Katz MH, Fleming JB, Bouvet M, Endo I, Hoffman RM. Selective efficacy of zoledronic acid on metastasis in a patient-derived orthotopic xenograph (PDOX) nude-mouse model of human pancreatic cancer. J Surg Oncol 2015; 111:311-5; PMID:25394368; https://doi.org/10.1002/jso.23816

[12] Fu X, Le P, Hoffman RM. A metastatic-orthotopic transplant nude-mouse model of human patient breast cancer. Anticancer Res 1993; 13:901-4; PMID:8352558

[13] Fu X, Hoffman RM. Human ovarian carcinoma metastatic models constructed in nude mice by orthotopic transplantation of histologically-intact patient specimens. Anticancer Res 1993; 13:283-6; PMID:8517640

[14] Wang X, Fu X, Hoffman RM. A new patient-like metastatic model of human lung cancer constructed orthotopically with intact tissue via thoracotomy in immunodeficient mice. Int J Cancer 1992; 51:992-5; PMID:1639545; https://doi.org/10.1002/ijc.2910510621

[15] Hiroshima Y, Zhang Y, Zhang M, Maawy A, Mii S, Yamamoto M, Uehara F, Miwa S, Yano S, Murakami T, et al. Establishment of a patient-derived orthotopic xenograph (PDOX) model of HER-2-positive cervical cancer expressing the clinical metastatic pattern. PLOS ONE 2015; 10:e0117417; PMID:25689852; https://doi.org/10.1371/journal.pone.0117417

[16] Fu X, Besterman JM, Monosov A, Hoffman RM. Models of human metastatic colon cancer in nude mice orthotopically constructed by using histologically intact patient specimens. Proc Natl Acad Sci USA 1991; 88:9345-9; PMID:1924398; https://doi.org/10.1073/pnas.88.20.9345

[17] Metildi CA, Kaushal S, Luiken GA, Talamini MA, Hoffman RM, Bouvet M. Fluorescently-labeled chimeric anti-CEA antibody improves detection and resection of human colon cancer in a patient-derived orthotopic xenograft (PDOX) nude mouse model. J Surg Oncol 2014; 109:451-8; PMID:24249594; https://doi.org/10.1002/jso.23507

[18] Hiroshima Y, Maawy A, Metildi CA, Zhang Y, Uehara F, Miwa S, Yano S, Sato S, Murakami T, Momiyama M, et al. Successful fluorescence-guided surgery on human colon cancer patient-derived orthotopic xenograft mouse models using a fluorophore-conjugated anti-CEA antibody and a portable imaging system. J Laparoendosc Adv Surg Tech A 2014; 24:241-7; PMID:24494971; https://doi.org/10.1089/lap.2013.0418

[19] Furukawa T, Kubota T, Watanabe M, Kitajima M, Fu X, Hoffman RM. Orthotopic transplantation of histologically intact clinical specimens of stomach cancer to nude mice: correlation of metastatic sites in mouse and individual patient donors. Int J Cancer 1993; 53:608-12; PMID:8436434; https://doi.org/10.1002/ijc.2910530414

[20] Murakami T, DeLong J, Eilber FC, Zhao M, Zhang Y, Zhang N, Singh A, Russell T, Deng S, Reynoso J, et al. Tumor-targeting *Salmonella typhimurium* A1-R in combination with doxorubicin eradicate soft tissue sarcoma in a patient-derived orthotopic xenograft PDOX model. Oncotarget 2016; 7:12783-90; PMID:26859573

[21] Hiroshima Y, Zhao M, Zhang Y, Zhang N, Maawy A, Murakami T, Mii S, Uehara F, Yamamoto M, Miwa S, et al. Tumor-targeting *Salmonella typhimurium* A1-R arrests a chemo-resistant patient soft-tissue sarcoma in nude mice. PLoS One 2015; 10:e0134324; PMID:26237416; https://doi.org/10.1371/journal.pone.0134324

[22] Kiyuna T, Murakami T, Tome Y, Kawaguchi K, Igarashi K, Zhang Y, Zhao M, Li Y, Bouvet M, Kanaya F, et al. High efficacy of tumor-targeting *Salmonella typhimurium* A1-R on a doxorubicin- and dactolisib-resistant follicular dendritic-cell sarcoma in a patient-derived orthotopic xenograft PDOX nude mouse model. Oncotarget 2016; 7:33046-54; PMID:27105519

[23] Murakami T, Singh AS, Kiyuna T, Dry SM, Li Y, James AW, Igarashi K, Kawaguchi K, DeLong JC, Zhang Y, et al. Effective molecular targeting of CDK4/6 and IGF-1R in a rare FUS-ERG fusion CDKN2A-deletion doxorubicin-resistant Ewing's sarcoma in a patient-derived orthotopic xenograft (PDOX) nude-mouse model. Oncotarget 2016; 7:47556-64

[24] Hiroshima Y, Zhang Y, Zhang N, Uehara F, Maawy A, Murakami T, Mii S, Yamamoto M, Miwa S, Yano S, et al. Patient-derived orthotopic xenograft (PDOX) nude mouse model of soft-tissue sarcoma more closely mimics the patient behavior in contrast to the subcutaneous ectopic model. Anticancer Res 2015; 35:697-701; PMID:25667448

[25] Yamamoto M, Zhao M, Hiroshima Y, Zhang Y, Shurell E, Eilber FC, Bouvet M, Noda M, Hoffman RM. Efficacy of tumor-targeting *Salmonella typhimurium* A1-R on a melanoma patient-derived orthotopic xenograft (PDOX) nude-mouse model. PLoS One 2016; 11:e0160882; PMID:27500926; https://doi.org/10.1371/journal.pone.0160882

[26] Kawaguchi K, Murakami T, Chmielowski B, Igarashi K, Kiyuna T, Unno M, Nelson SD, Russell TA, Dry SM, Li Y, et al. Vemurafenib-resistant BRAF-V600E mutated melanoma is regressed by MEK targeting drug trametinib, but not cobimetinib in a patient-derived orthotopic xenograft (PDOX) mouse model. Oncotarget 2016; 7:71737-43; PMID:27690220

[27] Kawaguchi K, Igarashi K, Murakami T, Chmiewloski B, Kiyuna T, Zhao M, Zhang Y, Singh A, Unno M, Nelson SD, et al. Tumor-targeting *Salmonella typhimurium* A1-R combined with Temozolomide regresses malignant melanoma with a BRAF-V600 mutation in a patient-derived orthotopic xenograft (PDOX) model. Oncotarget 2016; 7:85929-36; PMID:27835903

[28] Hoffman RM. Patient-derived orthotopic xenografts: better mimic of metastasis than subcutaneous xenografts. Nature Reviews Cancer 2015; 15:451-52; PMID:26422835; https://doi.org/10.1038/nrc3972

[29] Suetsugu A, Katz M, Fleming J, Moriwaki H, Bouvet M, Saji S, Hoffman RM. Multi-color palette of fluorescent proteins for imaging the tumor microenvironment of orthotopic tumorgraft mouse models of clinical pancreatic cancer specimens. J Cell Biochem 2012; 113:2290-5; PMID:22573550; https://doi.org/10.1002/jcb.24099

[30] Suetsugu A, Katz M, Fleming J, Truty M, Thomas R, Saji S, Moriwaki H, Bouvet M, Hoffman RM. Imageable fluorescent metastasis resulting in transgenic GFP mice orthotopically implanted with human-patient primary pancreatic cancer specimens. Anticancer Res 2012; 32:1175-80; PMID:22493347

[31] Suetsugu A, Katz M, Fleming J, Truty M, Thomas R, Saji S, Moriwaki H, Bouvet M, Hoffman RM. Non-invasive fluorescent-protein imaging of orthotopic pancreatic-cancer-patient tumorgraft progression in nude mice. Anticancer Res 2012; 32:3063-8; PMID:22843874

[32] Kiyuna T, Murakami T, Tome Y, Igarashi K, Kawaguchi K, Russell T, Eckhardt MA, Crompton J, Singh A, Bernthal N, et al. Labeling the stroma of a patient-derived orthotopic xenograft (PDOX) mouse models of undifferentiated pleomorphic soft-tissue sarcoma with red

fluorescent protein for rapid non-invasive drug screening. J Cell Biochem 2017; 118:361-5
[33] Hoffman RM, Yang M. Whole-body imaging with fluorescent proteins. Nature Protocols 2006; 1:1429-38
[34] Yano S, Hiroshima Y, Maawy A, Kishimoto H, Suetsugu A, Miwa S, Toneri M, Yamamoto M, Katz MHG, Fleming JB, et al. Color-coding cancer and stromal cells with genetic reporters in a patient-derived orthotopic xenograft (PDOX) model of pancreatic cancer enhances fluorescence-guided surgery. Cancer Gene Therapy 2015; 22:344-50
[35] Blagosklonny MV. Matching targets for selective cancer therapy. Drug Discov Today 2003; 8:1104-7. PMID:14678733
[36] Blagosklonny MV. Teratogens as anti-cancer drugs. Cell Cycle 2005; 4:1518-21; PMID:16258270
[37] Blagosklonny MV. Treatment with inhibitors of caspases, that are substrates of drug ransporters, selectively permits chemotherapy-induced apoptosis in multidrug-resistant cells but protects normal cells. Leukemia 2001; 15:936-41; PMID:11417480
[38] Blagosklonny MV. Target for cancer therapy: proliferating cells or stem cells. Leukemia 2006; 20:385-91; PMID:16357832
[39] Apontes P, Leontieva OV, Demidenko ZN, Li F, Blagosklonny MV. Exploring long-term protection of normal human fibroblasts and epithelial cells from chemotherapy in cell culture. Oncotarget 2011; 2:222-33; PMID:21447859
[40] Blagosklonny MV. Tissue-selective therapy of cancer. Br J Cancer 2003; 89:1147-51; PMID:14520435
[41] Yang M, Reynoso J, Bouvet M, Hoffman RM. A transgenic red fluorescent protein-expressing nude mouse for color-coded imaging of the tumor microenvironment. J Cell Biochem 2009; 106:279-84; PMID:19097136
[42] Vintersten K, Monetti C, Gertsenstein M, Zhang P, Laszlo L, Biechele S, Nagy A. Mouse in red: red fluorescent protein expression in mouse ES cells, embryos, and adult animals. Genesis 2004; 40:241-6; PMID:15593332
[43] Hoffman RM, Yang M. Color-coded fluorescence imaging of tumor-host interactions. Nature Protocols 2006; 1:928-935
[44] Hoffman RM. Orthotopic metastatic mouse models for anticancer drug discovery and evaluation: a bridge to the clinic. Investigational New Drugs 1999; 17:343-59; PMID:10759402
[45] Yamauchi K, Yang M, Jiang P, Xu M, Yamamoto N, Tsuchiya H, Tomita K, Moossa AR, Bouvet M, Hoffman RM. Development of real-time subcellular dynamic multicolor imaging of cancer cell trafficking in live mice with a variable-magnification whole-mouse imaging system. Cancer Res 2006; 66:4208-14; PMID:16618743
[46] Kawaguchi K, Murakami T, Suetsugu A, Kiyuna T, Igarashi K, Hiroshima Y, Zhao M, Zhang Y, Bouvet M, Clary B, et al. High-efficacy targeting of colon-cancer liver metastasis with *Salmonella typhimurium* A1-R via intra-portal-vein injection in orthotopic nude-mouse models. Oncotarget 2017; 8:19065-73